Hindawi Publishing Corporation
The Scientific World Journal
Volume 2013, Article ID 541496, 6 pages
http://dx.doi.org/10.1155/2013/541496

Research Article

Effect of Intrinsic Point Defect on the Magnetic Properties of ZnO Nanowire

Jiangni Yun, Zhiyong Zhang, and Tieen Yin

School of Information Science and Technology, Northwest University, Xi'an 710127, China

Correspondence should be addressed to Jiangni Yun; niniyun@nwu.edu.cn

Received 5 September 2013; Accepted 14 November 2013

Academic Editors: C. Granata, C. Grimaldi, and G. Xing

The effect of intrinsic point defect on the magnetic properties of ZnO nanowire is investigated by the first-principles calculation based on the density functional theory (DFT). The calculated results reveal that the pure ZnO nanowire without intrinsic point defect is nonmagnetic and ZnO nanowire with V_O, Zn_i, O_i, O_{Zn}, or Zn_O point defect also is nonmagnetic. However, a strong spin splitting phenomenon is observed in ZnO nanowire with V_{Zn} defect sitting on the surface site. The Mulliken population analysis reveals that the oxygen atoms which are close to the V_{Zn} defect do major contribution to the magnetic moment. Partial density states calculation further suggests that the appearance of the half-metallic ferromagnetism in ZnO nanorod with V_{Zn} originates from the hybridization of the O2p states with Zn 3d states.

1. Introduction

Recently diluted magnetic semiconductors (DMSs) have attracted much attention due to their potential application in novel spintronic devices. Among these DMSs, low dimensional ZnO-based DMSs have been found to be promising for nanometer scale optomagnetics devices, optoelectronics devices, and biotechnology [1–15]. Many investigations have been reported regarding the intrinsic ferromagnetism in undoped one-dimensional ZnO nanomaterials [9–15]. However, these reports demonstrate controversial results. For example, Xing et al. [9] have reported that the room temperature ferromagnetism (RTFM) in undoped ZnO nanowire can be attributed to the large population of Vo, since they can initiate defect-related hybridization at the Fermi level and establish a long-range ferromagnetic ordering. Ghosh et al. [10] have found that V_{Zn} was responsible for the ferromagnetic behaviour in pure ZnO nanowire. Until now, the exact mechanism of intrinsic magnetism in undoped ZnO nanowire is still controversial. On the other hand, to reveal the origin of intrinsic magnetism in undoped ZnO, many theoretical calculations have been performed to study the roles of intrinsic point defects in ZnO [16–23]. These calculation results have made important contributions to the understanding of the roles of defects in ZnO and enriched the underlying knowledge of ZnO significantly. However, most of these calculations focused on the formation energies and transition levels [17, 18, 20, 23], which could not be detected directly in experiments. To date, the comprehensive investigation about the effect of intrinsic point defect on the magnetic properties of ZnO nanowire is lacking.

In this paper, we perform the first-principles calculation based on the density functional theory (DFT) to investigate the effect of intrinsic point defect on the magnetic properties of ZnO nanowire. The method we use offers the advantage of cost-efficient alternative to conventional ab initio methods in quantum chemistry. It gives results of a quality comparable to or even better than MP2 for a cost that is on the same order as Hartree-Fock. A further advantage of DFT is that it can be significantly more efficient than even traditional SCF theory. Also the robust electron ensemble DFT approach can be used for systems with partial occupancies.

From the results obtained from this paper, a better understanding of the mechanism of intrinsic magnetic properties in undoped ZnO nanowire with sufficient details can be estimated, and some helpful instructions can be provided for the growth of low dimensional ZnO-based DMSs. These results also imply a promising way to synthesize undoped ZnO nanowire with ferromagnetism and shed light on the fabrication of ZnO-based nanometer scale magnetic devices.

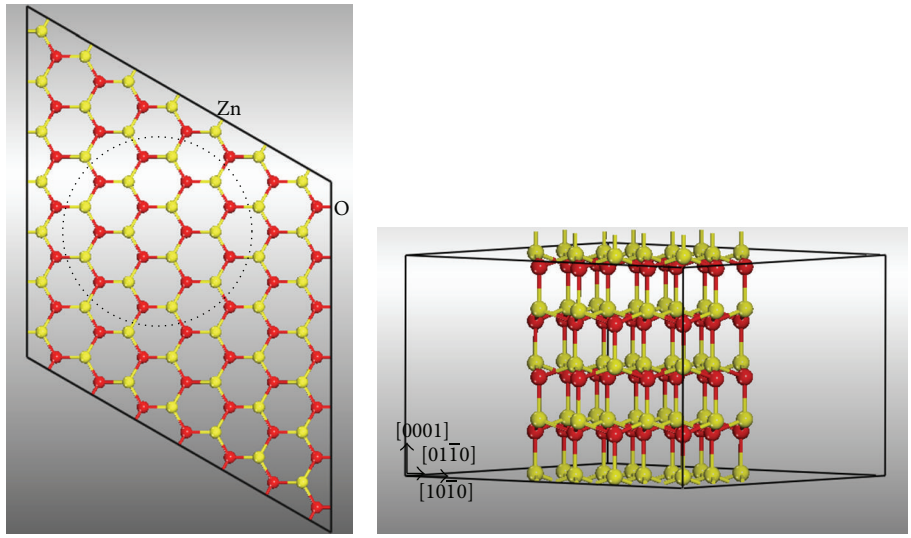

(a) (b)

Figure 1: (a) Top view of a 7 × 7 × 2 ZnO supercell with wurtzite structure, (b) $Zn_{48}O_{48}$ supercell which yields a nanowire along [0001] direction.

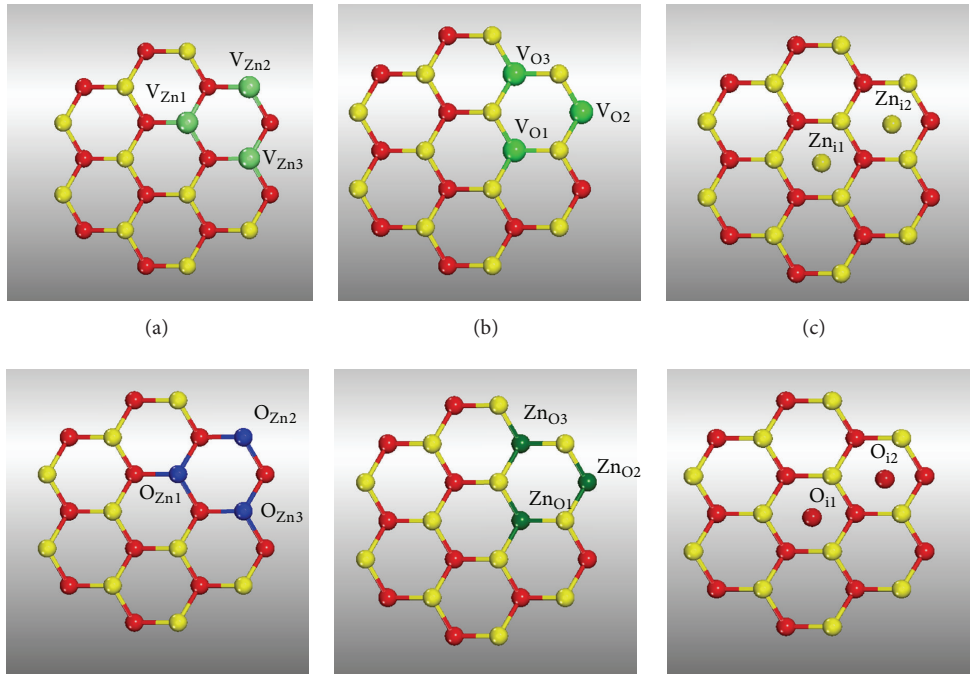

(a) (b) (c)

(d) (e) (f)

Figure 2: The configurations of ZnO nanowire (a) with V_{Zn}, (b) with V_O, (c) with Zn_i, (d) with O_{Zn}, (e) with Zn_O, and (f) with O_i defect.

2. Computational Details

As shown in Figure 1, the ZnO nanowire is generated from a 7 × 7 × 2 supercell of bulk wurtzite ZnO along the [0001] direction. It has a diameter of 1.0 nm, corresponding to 96 atoms per unit cell. A vacuum region of about 16 Å is set to avoid the interaction of the nanowire with its image. For the ZnO nanowire with V_{Zn}, V_O, O_{Zn}, or Zn_O defect, there are three inequivalent defect positions, which are denoted by V_{Zn1}–V_{Zn3}, V_{O1}–V_{O3}, O_{Zn1}–O_{Zn3}, and Zn_{O1}–Zn_{O3} as shown in Figures 2(a), 2(b), 2(d), and 2(e), respectively, whereas, there are two inequivalent Zn_i and O_i defect positions, which are denoted by Zn_{i1}-Zn_{i2} and O_{i1}-O_{i2} as shown in Figures 2(c) and 2(f), respectively.

All the calculations are performed by using the CASTEP software package [24]. The interaction between nuclei and

Table 1: Calculated relative energy $\Delta\varepsilon$ for the ZnO nanowire with different point defects (with the ground state energy taken as the reference value).

Defect	$\Delta\varepsilon$ (eV)
V_{Zn1}	0.12
V_{Zn2}	0.00
V_{Zn3}	0.04
O_{Zn1}	0.21
O_{Zn2}	0.00
O_{Zn3}	0.24
O_{i1}	0.00
O_{i2}	0.08
V_{O1}	1.01
V_{O2}	0.00
V_{O3}	0.66
Zn_{O1}	0.02
Zn_{O2}	0.00
Zn_{O3}	0.31
Zn_{i1}	0.00
Zn_{i2}	0.07

electrons is approximated with Vanderbilt ultrasoft pseudopotential [25] and the Perdew and Wang 91 parametrization [26] is taken as the exchange-correlation potential in the generalized gradient approximation (GGA). Plane wave basis with kinetic energy cutoff of 420 eV is used to represent wave functions. The Brillouin Zone integration is approximated using the special k-points sampling scheme of Monkhorst-Pack [27] and $1 \times 1 \times 16$ k-points grid is used. In order to obtain a stable structure, full relaxation is performed by using the BFGS algorithm [28] to minimize energy with respect to atomic position. The spin-polarized calculations are adopted to properly describe the electronic structure and magnetic properties of the constructed ZnO nanowire models. Each calculation is considered converged when the maximum root-mean-square convergent tolerance is less than 1×10^{-6} eV/atom.

With the settings described earlier, we have performed test calculations for bulk ZnO with wurtzite structure to verify the accuracy of the computational method. The obtained geometry optimization crystallographic parameters of wurtzite ZnO were $a = 3.248$ Å, $c = 5.206$ Å, and $c/a = 1.603$, which are in good agreement with the experimental values [29], $a = 3.250$ Å, $c = 5.207$ Å, and $c/a = 1.602$. We also tested the total energies and electronic structures of the considered defects model and the results indicate that the 96-atom supercell is sufficient for the present calculations.

3. Results and Discussion

3.1. Structural Stability. As shown in Figure 2, there are inequivalent defect positions in ZnO nanowire with intrinsic point defect. To determine the stable configurations for each intrinsic point defect, the relative energy $\Delta\varepsilon$ is calculated by comparing the total energy values of different configurations, with the ground state energy taken as the reference value. From the calculated relative energy $\Delta\varepsilon$ listed in Table 1, it is evident that the total energy of V_{Zn} at V_{Zn2} site is about 0.12 and 0.04 eV smaller than that at the V_{Zn1} and V_{Zn3} sites, respectively, and thus, the V_{Zn2} is the most stable site for V_{Zn} defect. Similar to V_{Zn}, the V_O, O_{Zn}, and Zn_O the also prefered at the V_{O2}, O_{Zn2}, and Zn_{O2} sites, respectively. While for the Zn_i and O_i defect, they are prefered at the Zn_{i1} and O_{i1} sites, respectively. Therefore, the magnetic properties of ZnO nanowire with intrinsic point defects are calculated based on the V_{Zn2}, V_{O2}, O_{Zn2}, Zn_{O2}, Zn_{i1}, and O_{i1} configurations. On the other hand, the V_{Zn2} and V_{Zn3} configurations are nearly degenerate in total energy, and the total energy of them is smaller than that of the V_{Zn1} configuration. This clearly suggests that the V_{Zn} defect shows selectivity of site occupancy and prefers sitting on the surface site.

3.2. Magnetic Properties. In this part, the electronic structures of ZnO nanowire without and with different intrinsic point defect will be discussed and compared with each other. Four indicators will be used to reveal the effect of intrinsic point defect on the magnetic properties of ZnO nanowire, which are the band structure (BS), total density of states (DOS), partial density of states (PDOS), and Mulliken population analysis. Each of these tools can demonstrate some aspects of structure features. For comparison, the BS, total DOS, and PDOS of ZnO nanowire without intrinsic point defect are calculated first and the results are shown in Figure 3.

As shown in Figure 3, the spin-up and spin-down DOSs of pure ZnO nanowire are completely symmetrical, indicating that the pure ZnO nanowire is nonmagnetic. Moreover, the ZnO nanowire has a direct band gap at the relatively high dispersion along the $\Gamma(0, 0, 0) \rightarrow Z(0, 0, 0.5)$ direction. The direct gap of 1.86 eV is in good agreement with that of the first-principles calculation by Yang et al. [30].

The total DOSs for spin-up and spin-down electrons of the ZnO nanowire with V_{Zn}, V_O, Zn_i, O_i, O_{Zn} or Zn_O point defect are plotted in Figure 4. Similar to the pure ZnO nanowire, the ZnO nanowire with V_O, Zn_i, O_i, O_{Zn}, or Zn_O point defect also is nonmagnetic. However, a strong spin splitting phenomenon is observed in the ZnO nanowire with V_{Zn} defect. The spin-up and spin-down DOSs are asymmetrical near the top of valence bands.

By analysis of the BS of spin-up and spin-down electrons of the ZnO nanowire with V_{Zn} defect shown in Figure 5, it is found that the Fermi level moves from the spin-up to the spin-down band. The system shows half-metallic behavior in which the spin-up and spin-down electrons possess a Fermi surface, in agreement with the previous report [21]. In addition, as shown in Figure 5(b), three defect-related acceptor energy levels appear near the top of the spin-down valence bands. The upper two acceptor energy levels are deep and highly localized. The lower one is partially occupied by the electrons and is highly localized. This result reveals that the hole of the acceptor level cannot be excited easily into the valence bands, and the V_{Zn} defect has little contribution to the p-type electrical activity of ZnO. Our conclusion confirms the

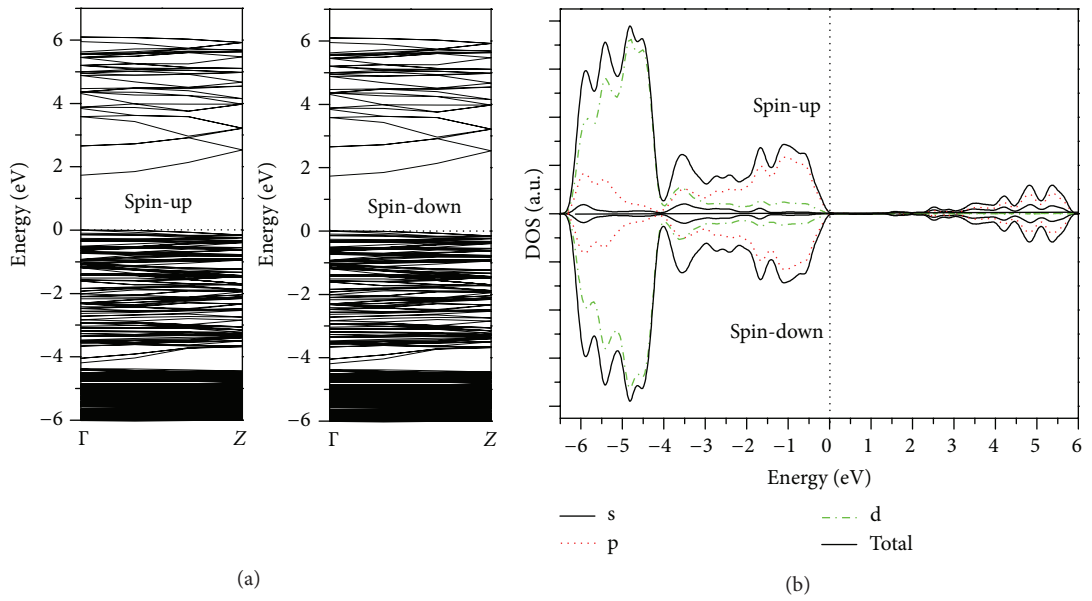

Figure 3: Calculated BS, total DOS, and PDOS of the pure ZnO nanowire. The Fermi level is set to zero on the energy scale, which will be adopted below unless otherwise stated.

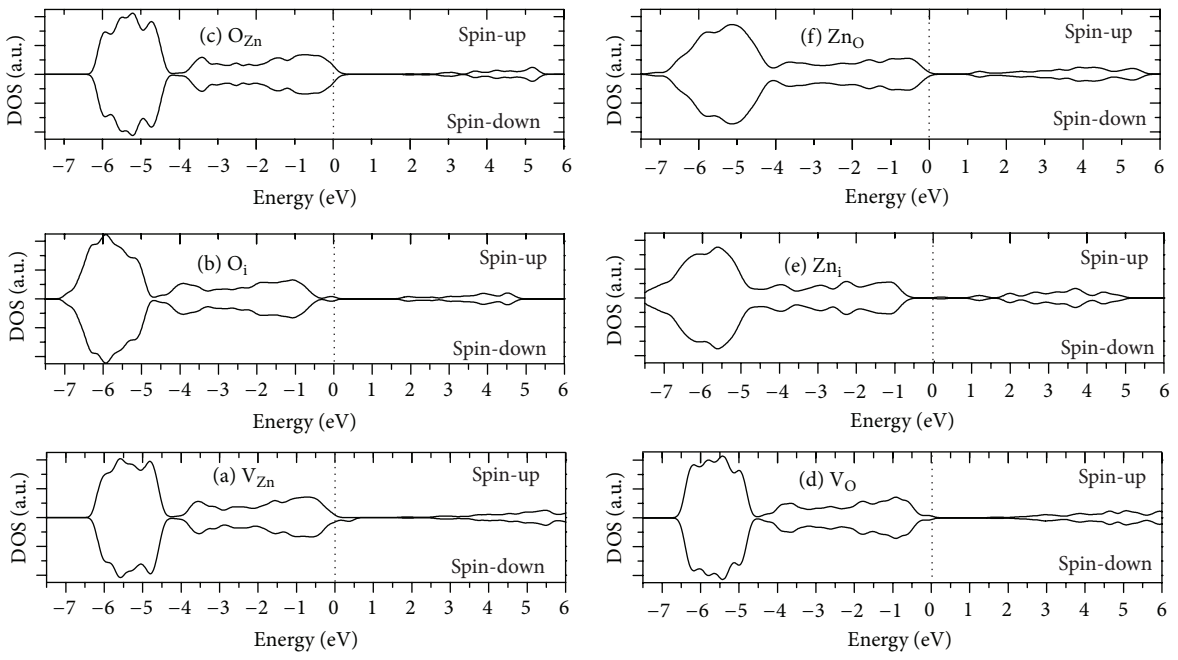

Figure 4: Calculated total DOS for ZnO nanowire with different intrinsic point defects.

experiment results that V_{Zn} defects play minor role in p-type conductivity of ZnO [31].

By further analysis of the PDOS shown in Figure 6, it can be found that the metallic spin-down DOS near the Fermi level is mainly composed of O2p and Zn 3d states. In particular, O2p states do major contribution to the magnetic moment. This suggests that the appearance of the half-metallic ferromagnetism in ZnO nanorod with V_{Zn} originates from the hybridization of the O2p states with Zn 3d states.

Furthermore, the calculated Mulliken population analysis of the ZnO nanowire with V_{Zn} defect is listed in Table 2. Evidently, the O atoms around the V_{Zn} make major contribution to the observed magnetic moment. Magnetic moment of $0.562\mu_B$, $0.556\mu_B$ and $0.557\mu_B$ is from each of the three O atoms in the basal plane and $0.102\mu_B$ from the O atom in the axial plane. The residual magnetic moment is from the neighboring Zn atoms of the V_{Zn}.

Structurally, at V_{Zn} in ZnO, there are four O atoms with dangling bonds pointing towards the vacancy site, where

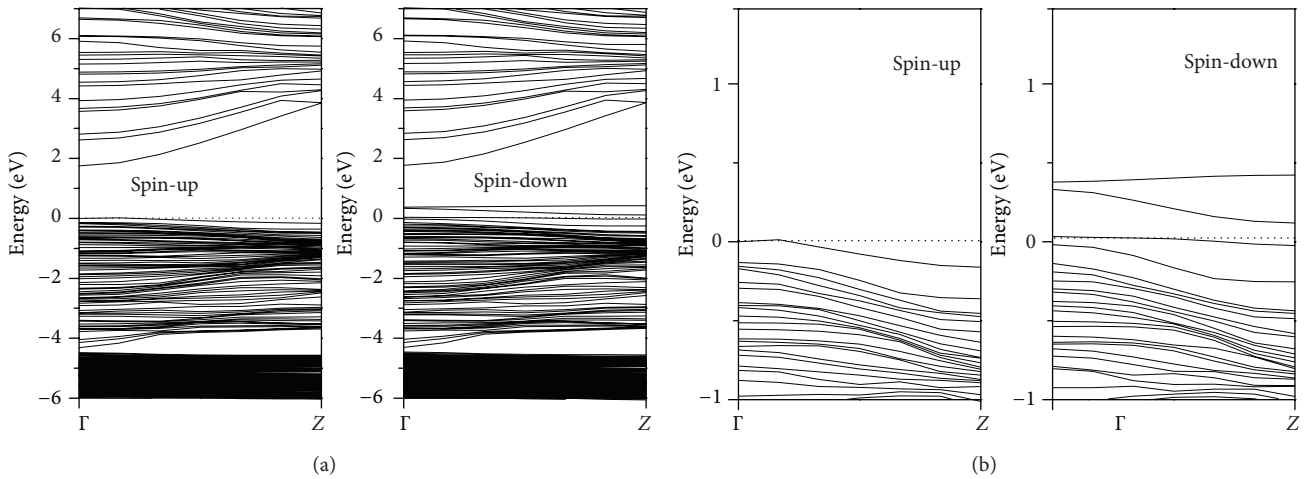

Figure 5: Calculated BS of ZnO nanowire with V_{Zn} defect. The corresponding BS near the Fermi level in Figure 5(a) is plotted in Figure 5(b).

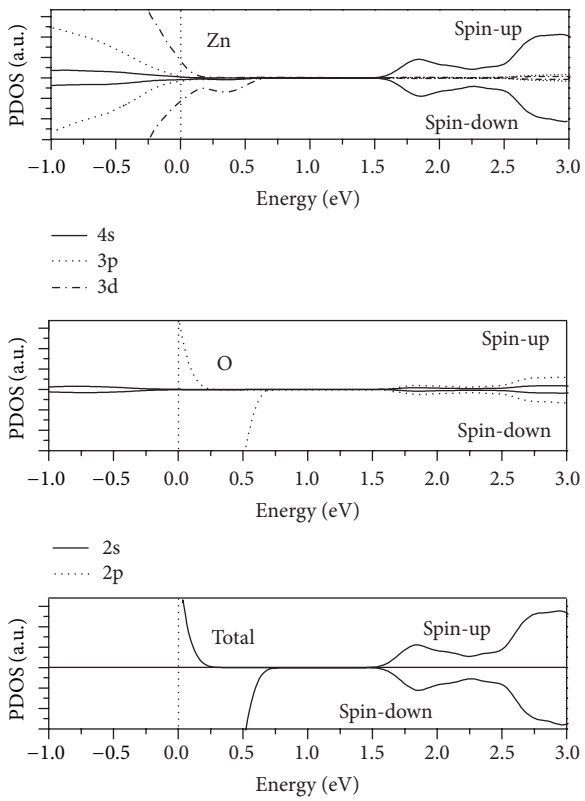

Figure 6: Calculated PDOS of ZnO nanowire with V_{Zn} defect.

the dangling bonds feature O2p states. When this system is neutral, each dangling bond holds 1/2 electrons and interacts with each other to lower the total energy of the whole system. In this case, because of the tetrahedral structure of the four O atoms, the interaction between the dangling bonds results in hybrid orbital splitting. Therefore, the O atoms around the V_{Zn} make major contribution to the observed magnetic moment.

Table 2: Calculated Mulliken population of the ZnO nanowire with V_{Zn} defect. Around the V_{Zn}, the O_{ai} represents the first-nearest neighboring O atoms in the basal plane, the O_c is the second-nearest neighboring O atoms in the axial plane, and the Zn_{ai} is the third-nearest neighboring Zn atoms in the basal plane.

Atom	μ_{total}/μ_B
O_{a1}	0.562
O_{a2}	0.556
O_{a3}	0.557
O_c	0.102
—	—
—	—
Zn_{a1}	0.006
Zn_{a2}	0.005
Zn_{a3}	0.001
Zn_{a4}	0.001
Zn_{a5}	0.001
Zn_{a6}	0.001

4. Conclusions

In conclusion, the effect of intrinsic point defect on the magnetic properties of ZnO nanowire is investigated by the first-principles calculation based on the DFT. The calculated BS, DOS, PDOS, and Mulliken population analysis results reveal that the pure ZnO nanowire without intrinsic point defect is nonmagnetic and ZnO nanowire with V_O, Zn_i, O_i, O_{Zn}, or Zn_O point defect also is nonmagnetic. However, a strong spin splitting phenomenon is observed in ZnO nanowire with V_{Zn} defect sitting on the surface site. At V_{Zn} in ZnO, there are four O atoms with dangling bonds pointing towards the vacancy site. Because of the tetrahedral structure of the four O atoms, the interaction between the dangling bonds results in hybrid orbital splitting.

Acknowledgments

This work is supported by the Natural Science Basic Research Plan in Shaanxi Province of China (Program no. 2011JQ8034), the Science and Technology Star Project of Shaanxi Province (2013KJXX-24), the Open Foundation of Key Laboratory of Photoelectronic Technology of Shaanxi Province (Grant no. ZS11009), the Science Foundation of Northwest University (nos. 10NW08, PR10069), and the NWU Graduate Innovation and Creativity Funds (YZZ12098). The authors also acknowledge the support of the Scientific Research Program Funded by Shaanxi Provincial Education Department (Program no. 11JK0831).

References

[1] M. J. Xin, Y. Q. Chen, C. Jia, and X. H. Zhang, "Electrocodeposition synthesis and room temperature ferromagnetic anisotropy of high concentration Fe-doped ZnO nanowire arrays," *Materials Letters*, vol. 62, no. 17–18, pp. 2717–2720, 2008.

[2] F. Ahmed, S. Kumar, N. Arshi, M. S. Anwar, B. H. Koo, and C. G. Lee, "Defect induced room temperature ferromagnetism in well-aligned ZnO nanorods grown on Si (100) substrate," *Thin Solid Films*, vol. 519, no. 23, pp. 8199–8202, 2011.

[3] F. Li, C. W. Zhang, P. J. Wang, and P. Li, "Theoretical studies of the magnetism of the first-row adatom on the ZnO nanotube," *Applied Surface Science*, vol. 258, no. 17, pp. 6621–6626, 2012.

[4] S. Yılmaz, J. Nisar, Y. Atasoy et al., "Defect-induced room temperature ferromagnetism in B-doped ZnO," *Ceramics International*, vol. 39, no. 4, pp. 4609–4617, 2013.

[5] H. L. Shi and Y. F. Duan, "Magnetic coupling properties of Mn-doped ZnO nanowires: first-principles calculations," *Journal of Applied Physics*, vol. 103, Article ID 073903, 2008.

[6] Q. Wang, Q. Sun, and P. Jena, "Ferromagnetism in Mn-Doped GaN nanowires," *Physical Review Letters*, vol. 95, Article ID 167202, 2005.

[7] Q. Wang, Q. Sun, P. Jena, Z. Hu, R. Note, and Y. Kawazoe, "First-principles study of magnetic properties in V-doped ZnO," *Applied Physics Letters*, vol. 91, Article ID 063116, 2007.

[8] F. C. Zhang, J. T. Dong, W. H. Zhang, and Z. Y. Zhang, "Ferromagnetism of V-doped ZnO nanowires," *Chinese Physics B*, vol. 22, no. 2, Article ID 027503, 2013.

[9] G. Z. Xing, D. D. Wang, J. B. Yi et al., "Correlated d^0 ferromagnetism and photoluminescence in undoped ZnO nanowires," *Applied Physics Letters*, vol. 96, no. 11, Article ID 112511, 2010.

[10] S. Ghosh, G. G. Khan, and K. Mandal, " d0 Ferromagnetism in Oxide Nanowires: Role of Intrinsic Defects," *European PhysicalJournal*, vol. 40, Article ID 03001, 2013.

[11] F. Gao, J. F. Hu, J. H. Wang, C. L. Yang, and H. W. Qin, "Ferromagnetism induced by intrinsic defects and carbon substitution in single-walled ZnO nanotube," *Chemical Physics Letters*, vol. 488, no. 1–3, pp. 57–61, 2010.

[12] X. Y. Xu, C. X. Xu, J. Dai, J. G. Hu, F. J. Li, and S. Zhang, "Size dependence of defect-induced room temperature ferromagnetism in undoped ZnO nanoparticles," *The Journal of Physical Chemistry C*, vol. 116, no. 15, pp. 8813–8818, 2012.

[13] M. V. Limaye, S. B. Singh, R. Das, P. Poddar, and S. K. Kulkarni, "Room temperature ferromagnetism in undoped and Fe doped ZnO nanorods: microwave-assisted synthesis," *Journal of Solid State Chemistry*, vol. 184, no. 2, pp. 391–400, 2011.

[14] J.-I. Hong, J. Choi, S. S. Jang et al., "Magnetism in dopant-free ZnO nanoplates," *Nano Letters*, vol. 12, no. 2, pp. 576–581, 2012.

[15] C. Peng, Y. Liang, K. Wang, Y. Zhang, G. Zhao, and Y. Wang, "Possible origin of ferromagnetism in an undoped ZnO d0 semiconductor," *Journal of Physical Chemistry C*, vol. 116, no. 17, pp. 9709–9715, 2012.

[16] Q. Wang, Q. Sun, G. Chen, Y. Kawazoe, and P. Jena, "Vacancy-induced magnetism in ZnO thin films and nanowires," *Physical Review B*, vol. 77, Article ID 205411, 2008.

[17] A. F. Kohan, G. Ceder, D. Morgan, and C. G. Van De Walle, "First-principles study of native point defects in ZnO," *Physical Review B*, vol. 61, no. 22, pp. 15019–15027, 2000.

[18] C. H. Patterson, "Role of defects in ferromagnetism in $Zn_{1-x}Co_xO$: a hybrid density-functional study," *Physical Review B*, vol. 74, Article ID 144432, 2006.

[19] J. Hu and B. C. Pan, "Electronic structures of defects in ZnO: hybrid density functional studies," *Journal of Chemical Physics*, vol. 129, Article ID 154706, 2008.

[20] P. Erhart, K. Albe, and A. Klein, "First-principles study of intrinsic point defects in ZnO: role of band structure, volume relaxation, and finite-size effects," *Physical Review B*, vol. 73, Article ID 205203, 2006.

[21] T. Chanier, I. Opahle, M. Sargolzaei, R. Hayn, and M. Lannoo, "Magnetic state around cation vacancies in IIâ"VI semiconductors," *Physical Review Letters*, vol. 100, no. 2, Article ID 026405, 2008.

[22] J. Hu and B. C. Pan, "The optical and vibrational properties of dominant defects in undoped ZnO: a first-principles study," *Journal of Applied Physics*, vol. 105, Article ID 083710, 2009.

[23] A. Janotti and C. G. Van de Walle, "Native point defects in ZnO," *Physical Review B*, vol. 76, Article ID 165202, 2007.

[24] M. D. Segall, P. J. D. Lindan, M. J. Probert et al., "First-principles simulation: ideas, illustrations and the CASTEP code," *Journal of Physics Condensed Matter*, vol. 14, no. 11, pp. 2717–2744, 2002.

[25] D. Vanderbilt, "Soft self-consistent pseudopotentials in a generalized eigenvalue formalism," *Physical Review B*, vol. 41, pp. 7892–7895, 1990.

[26] J. P. Perdew, J. A. Chevary, S. H. Vosko et al., "Atoms, molecules, solids, and surfaces: applications of the generalized gradient approximation for exchange and correlation," *Physical Review B*, vol. 46, no. 11, pp. 6671–6687, 1992.

[27] H. J. Monkhorst and J. D. Pack, "Special points for Brillouin-zone integrations," *Physical Review B*, vol. 13, no. 12, pp. 5188–5192, 1976.

[28] B. G. Pfrommer, M. Côté, S. G. Louie, and M. L. Cohen, "Relaxation of crystals with the quasi-newton method," *Journal of Computational Physics*, vol. 131, no. 1, pp. 233–240, 1997.

[29] J. Albertsson, S. C. Abrahams, and A. Kvick, "Atomic displacement, anharmonic thermal vibration, expansivity and pyroelectric coefficient thermal dependences in ZnO," *Acta Crystallographica*, vol. 45, pp. 34–40, 1989.

[30] Y. R. Yang, X. H. Yan, Y. Xiao, and Z. H. Guo, "The optical properties of one-dimensional ZnO: a first-principles study," *Chemical Physics Letters*, vol. 446, no. 1–3, pp. 98–102, 2007.

[31] S. Duttaa, S. Chattopadhyayb, A. Sarkarc, M. Chakrabartid, D. Sanyald, and D. Janaa, "Role of defects in tailoring structural, electrical and optical properties of ZnO," *Progress in Materials Science*, vol. 54, no. 1, pp. 89–136, 2009.